



# Application of a detailed biomass pyrolysis kinetic scheme to hardwood and softwood torrefaction



Andrés Anca-Couce<sup>a,\*</sup>, Ingwald Obernberger<sup>a,b</sup>

<sup>a</sup>Institute for Process and Particle Engineering, Graz University of Technology, Inffeldgasse 21b, 8010 Graz, Austria

<sup>b</sup>BIOS BIOENERGIESYSTEME GmbH, Inffeldgasse 21b, 8010 Graz, Austria

## ARTICLE INFO

### Article history:

Received 20 May 2015

Received in revised form 13 November 2015

Accepted 17 November 2015

Available online 25 November 2015

### Keywords:

Torrefaction  
Kinetic scheme  
Biomass  
Hardwood  
Softwood

## ABSTRACT

A detailed pyrolysis kinetic scheme is applied in this work for biomass torrefaction, with a focus on hardwood and softwood. The scheme includes secondary charring reactions, relevant for particles of a certain thickness, and sugar formation is avoided due to the catalytic effect of alkali metals in biomass. The release of acetic acid from hardwood and softwood hemicellulose is also considered. Representative initial compositions of hardwood and softwood are proposed in order to correctly predict mass loss in pyrolysis and torrefaction micro-TGA experiments. The predictions for product composition are validated with torrefaction batch experiments conducted in a lab-scale reactor with beech and spruce. The scheme predicts with good accuracy the yields of permanent gases and the main groups in which the condensable species are classified. The amount of secondary charring reactions is higher in the lab-scale than in the micro-TGA experiments, due to the higher particle size. The main discrepancies can be explained by the limitations of the scheme: reactive drying is not included and xylan is considered as representative for hemicellulose, which leads to deviations in the predictions of some products from softwood, e.g. furans. A more precise description of hemicellulose from softwood would include a hemicellulose reaction scheme based on glucomannan.

© 2015 Elsevier Ltd. All rights reserved.

## 1. Introduction

Biomass, as other renewable energy sources, is expected to play a more important role in the energy mix of the future. Torrefaction is a mild pyrolysis process at temperatures ranging from 220 to 350 °C where mainly the hemicellulose fraction decomposes. Torrefaction and its applications were reviewed by Van der Stelt et al. [1] and Tumuluru et al. [2]. In this process biomass loses mass and gets enriched in carbon due to volatiles release. Additionally, torrefaction improves grindability, increases hydrophobicity and reduces biological and thermal degradation, which improves storage and transportation properties. Due to these benefits torrefaction may become an interesting biomass pre-treatment technology.

Torrefaction is usually modelled with a two steps kinetic scheme [3–5] where there is at each step a competition between formation of volatiles and solid products. This scheme is inspired from the one developed for hemicellulose by Di Blasi and Lanzetta [6]. The composition of the volatiles of each reaction was

\* Corresponding author. Tel.: +43 (0) 316 873 30432; fax: +43 (0) 316 873 1030432.

E-mail address: [anca-couce@tugraz.at](mailto:anca-couce@tugraz.at) (A. Anca-Couce).

calculated by Bates and Ghoniem [7] for a hardwood species (willow), based on the kinetics [3] and analysis of products [8] from Prins et al. The main limitation of this scheme is that it can just be applied for biomass species for which the kinetics and product composition were calculated, i.e. it cannot be generally applied for lignocellulosic biomass. Moreover, the competition between the production of char and volatiles is described with different activation energies for each reaction, not considering other relevant parameters in charring as particle size, pressure or ash content [9].

Biomass pyrolysis kinetics based on the sum of the contributions of the components hemicellulose, cellulose and lignin were also employed to describe mass loss in torrefaction [10,11]. A kinetic scheme which is able to predict biomass pyrolysis should also be valid for biomass torrefaction, as this is just a partial pyrolysis process. The authors of this paper applied a detailed kinetic scheme of biomass pyrolysis [9,12] to predict the product composition of torrefaction of beech (hardwood) chips [13]. The objective of this work is to present a general kinetic scheme which is able to generally predict mass loss evolution and product composition of torrefaction of lignocellulosic biomass. This kinetic scheme will be applied for hardwood and softwood torrefaction in this work. The kinetic scheme is presented in Section 2, mass loss evolution

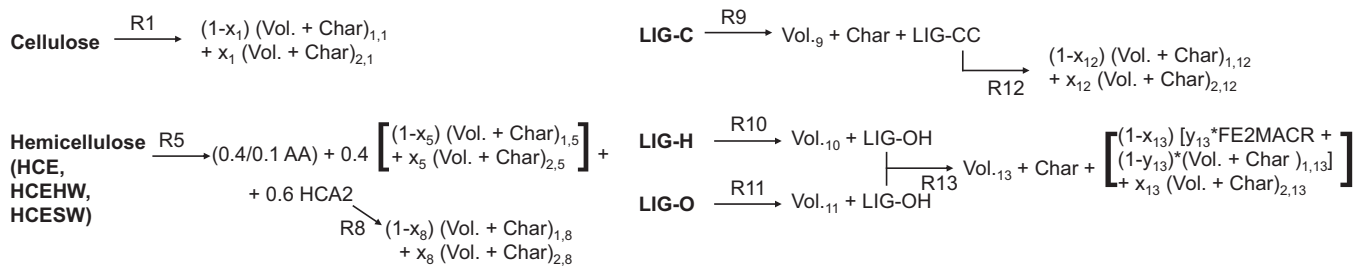


Fig. 1. Summary of the adapted reaction scheme. The release of acetic acid (AA) from hemicellulose is different for hardwood and softwood.

is discussed in Section 3 and product composition in Section 4. Finally, the conclusions are exposed.

## 2. Kinetic scheme

The pyrolysis kinetic scheme presented in this work to model biomass torrefaction is going to be briefly described. It is based on the scheme developed by Ranzi et al. [12] for pyrolysis of small ash free biomass particles (i.e., primary pyrolysis) called from now on original scheme. A recent update of this scheme, which has not been employed in this work, was presented by Corbetta et al. [14]. Biomass consists of cellulose, hemicellulose and 3 types of lignin which independently decompose and the volatiles are represented by 20 species, including main permanent gases and condensable species. This original scheme was adapted by the authors of this paper [9] to include the presence of secondary char formation reactions, which are relevant for particles of a certain thickness as under typical torrefaction conditions. In these reactions char is produced together with other products, such as  $\text{H}_2\text{O}$  and  $\text{CO}_2$ , from the original products of primary pyrolysis. Moreover, in the competition between fragmentation and sugar formation reactions, the catalytic effect of alkali metals in biomass, together with the presence of secondary reactions of the volatiles in particles of a certain thickness, leads to the preference of the fragmentation pathway over sugar formation for both cellulose and hemicellulose in the adaptation.

The employed adapted scheme is summarized in Fig. 1, the reactions are detailed in Table 1 and the list of species is shown in Table 2. Cellulose pyrolysis is described with one reaction representing devolatilization through ring fragmentation plus a secondary reaction representing charring. An adjustable parameter “ $x_1$ ” represents the amount of the initial fragmentation primary products –  $(\text{Vol.} + \text{Char})_{1,1}$ , including several low molecular weight compounds such as hydroxyacetaldehyde (HAA), 5-hydroxymethyl-furfural (HMFU),  $\text{CO}_2$  or  $\text{H}_2\text{O}$  – that react to form the secondary products –  $(\text{Vol.} + \text{Char})_{2,1}$ , including char,  $\text{H}_2\text{O}$ ,  $\text{CO}_2$  and  $\text{H}_2$ . The hemicellulose scheme is based on pyrolysis of xylan, which is a good representative of the hemicelluloses of hardwoods. It consists of two successive reactions. The scheme of lignin consists of three different components: LIG-C, LIG-H and LIG-O, which are richer in carbon, hydrogen and oxygen, respectively. Hemicellulose and lignin pyrolysis in the adapted scheme also include adjustable parameters “ $x_i$ ” representing the amount of secondary charring reactions. These parameters should depend on the retention time and partial pressure of the volatiles in the particle, presence of minerals and temperature. A value in the range of 0.3–0.4, constant for all components, provided good results for slow pyrolysis in fixed beds of wood particles with a size of around 1 cm [9].

In this scheme char is not just produced as pure carbon, but also as several  $G\{\}$  forms ( $G\{\text{CO}_2\}$ ,  $G\{\text{CO}\}$ ,  $G\{\text{COH}_2\}$ ) and  $G\{\text{H}_2\}$ ) that further react at higher temperatures producing  $\text{CO}_2$ ,  $\text{CO}$  or  $\text{H}_2$ , but these reactions are not active at typical torrefaction temperatures.

Table 1

List of reactions of the adapted scheme (SW: softwood, HW: hardwood).

Reaction		$A$ ( $\text{s}^{-1}$ )	$E$ (kJ/mol)	
1	CELL	$\rightarrow (1-x_1) * (0.95 \text{ HAA} + 0.25 \text{ GLYOX} + 0.2 \text{ CH}_3\text{CHO} + 0.25 \text{ HMFU} + 0.2 \text{ C}_3\text{H}_6\text{O} + 0.16 \text{ CO}_2 + 0.23 \text{ CO} + 0.9 \text{ H}_2\text{O} + 0.1 \text{ CH}_4 + 0.61 \text{ Char}) + x_1 * (5.5 \text{ Char} + 4 \text{ H}_2\text{O} + 0.5 \text{ CO}_2 + \text{H}_2)$	$8 \times 10^{13}$	192.5
5	HCE	$\rightarrow 0.4 * [(1-x_5) * (0.75 \text{ G}\{\text{H}_2\} + 0.8 \text{ CO}_2 + 1.4 \text{ CO} + 0.5 \text{ CH}_2\text{O} + 0.25 \text{ CH}_3\text{OH} + 0.125 \text{ ETOH} + 0.125 \text{ H}_2\text{O} + 0.625 \text{ CH}_4 + 0.25 \text{ C}_2\text{H}_4 + 0.675 \text{ Char}) + x_5 * (4.5 \text{ Char} + 3 \text{ H}_2\text{O} + 0.5 \text{ CO}_2 + \text{H}_2)] + 0.6 \text{ HCEA2}$	$1 \times 10^{10}$	129.7
5 (HW)	HCEHW	$\rightarrow 0.4 \text{ AA} + 0.4 * [(1-x_5) * (0.75 \text{ G}\{\text{H}_2\} + 0.8 \text{ CO}_2 + 1.4 \text{ CO} + 0.5 \text{ CH}_2\text{O} + 0.25 \text{ CH}_3\text{OH} + 0.125 \text{ ETOH} + 0.125 \text{ H}_2\text{O} + 0.625 \text{ CH}_4 + 0.25 \text{ C}_2\text{H}_4 + 0.675 \text{ Char}) + x_5 * (4.5 \text{ Char} + 3 \text{ H}_2\text{O} + 0.5 \text{ CO}_2 + \text{H}_2)] + 0.6 \text{ HCEA2}$	$1 \times 10^{10}$	129.7
5 (SW)	HCESW	$\rightarrow 0.1 \text{ AA} + 0.4 * [(1-x_5) * (0.75 \text{ G}\{\text{H}_2\} + 0.8 \text{ CO}_2 + 1.4 \text{ CO} + 0.5 \text{ CH}_2\text{O} + 0.25 \text{ CH}_3\text{OH} + 0.125 \text{ ETOH} + 0.125 \text{ H}_2\text{O} + 0.625 \text{ CH}_4 + 0.25 \text{ C}_2\text{H}_4 + 0.675 \text{ Char}) + x_5 * (4.5 \text{ Char} + 3 \text{ H}_2\text{O} + 0.5 \text{ CO}_2 + \text{H}_2)] + 0.6 \text{ HCEA2}$	$1 \times 10^{10}$	129.7
8	HCEA2	$\rightarrow (1-x_8) * (0.2 \text{ CO}_2 + 0.5 \text{ CH}_4 + 0.25 \text{ C}_2\text{H}_4 + 0.8 \text{ G}\{\text{CO}_2\} + 0.8 \text{ G}\{\text{COH}_2\} + 0.7 \text{ CH}_2\text{O} + 0.25 \text{ CH}_3\text{OH} + 0.125 \text{ ETOH} + 0.125 \text{ H}_2\text{O} + \text{Char}) + x_8 * (4.5 \text{ Char} + 3 \text{ H}_2\text{O} + 0.5 \text{ CO}_2 + \text{H}_2)$	$1 \times 10^{10}$	138.1
9	LIG-C	$\rightarrow 0.35 \text{ LIG-CC} + 0.1 \text{ pCOUMARYL} + 0.08 \text{ PHENOL} + 0.41 \text{ C}_2\text{H}_4 + \text{H}_2\text{O} + 0.495 \text{ CH}_4 + 0.32 \text{ CO} + \text{G}\{\text{COH}_2\} + 5.735 \text{ Char}$	$4 \times 10^{15}$	202.9
10	LIG-H	$\rightarrow \text{LIG-OH} + \text{C}_3\text{H}_6\text{O}$	$2 \times 10^{13}$	156.9
11	LIG-O	$\rightarrow \text{LIG-OH} + \text{CO}_2$	$1 \times 10^9$	106.7
12	LIG-CC	$\rightarrow (1-x_{12}) * (0.3 \text{ pCOUMARYL} + 0.2 \text{ PHENOL} + 0.35 \text{ C}_3\text{H}_4\text{O}_2 + 0.7 \text{ H}_2\text{O} + 0.65 \text{ CH}_4 + 0.6 \text{ C}_2\text{H}_4 + \text{G}\{\text{COH}_2\} + 0.8 \text{ G}\{\text{CO}\} + 6.4 \text{ Char}) + x_{12} * (14.5 \text{ Char} + 3 \text{ H}_2\text{O} + 0.5 \text{ CO}_2 + 4 \text{ H}_2)$	$5 \times 10^6$	131.8
13	LIG-OH	$\rightarrow \text{H}_2\text{O} + \text{CH}_3\text{OH} + 0.45 \text{ CH}_4 + 0.2 \text{ C}_2\text{H}_4 + 1.4 \text{ G}\{\text{CO}\} + 0.6 \text{ G}\{\text{COH}_2\} + 0.1 \text{ G}\{\text{H}_2\} + 4.15 \text{ Char} + [(1-x_{13}) * (y_{13}/100 * \text{FE2MACR} + (1-y_{13}/100) * (\text{H}_2\text{O} + 0.5 \text{ CO} + 0.2 \text{ CH}_2\text{O} + 0.4 \text{ CH}_3\text{OH} + 0.2 \text{ CH}_3\text{CHO} + 0.2 \text{ C}_3\text{H}_6\text{O} + 0.6 \text{ CH}_4 + 0.65 \text{ C}_2\text{H}_4 + \text{G}\{\text{CO}\} + 0.5 \text{ G}\{\text{COH}_2\} + 5.5 \text{ Char})) + x_{13} * (10.5 \text{ Char} + 3 \text{ H}_2\text{O} + 0.5 \text{ CO}_2 + 3 \text{ H}_2)]$ $y_{13} = -3.6800\text{E}-11 * T^5 + 8.2619\text{E}-08 * T^4 - 6.8901\text{E}-05 * T^3 + 2.6124\text{E}-02 * T^2 - 4.5911 * T + 4.0398\text{E} + 02; T \text{ in } [^\circ\text{C}]$	$3 \times 10^8$	125.5
16	$\text{G}\{\text{CO}_2\}$	$\rightarrow \text{CO}_2$	$1 \times 10^5$	100.4
17	$\text{G}\{\text{CO}\}$	$\rightarrow \text{CO}$	$1 \times 10^{13}$	209.2
18	$\text{G}\{\text{COH}_2\}$	$\rightarrow \text{CO} + \text{H}_2$	$5 \times 10^{11}$	272.0
19	$\text{G}\{\text{H}_2\}$	$\rightarrow \text{H}_2$	$5 \times 10^{11}$	313.8

**Table 2**  
List of species.

Abbreviation	Name	Atomic composition	Group
<i>Solids</i>			
CELL	Cellulose	$C_6H_{10}O_5$	
HCE	Hemicellulose	$C_5H_8O_4$	
HCEHW	Hemicellulose for hardwoods	$10 * (C_5H_8O_4) + 4 * (C_2H_4O_2)$	
HCESW	Hemicellulose for softwoods	$10 * (C_5H_8O_4) + 1 * (C_2H_4O_2)$	
HCEA2	Activated hemicellulose 2	$C_5H_8O_4$	
LIG-C	Carbon-rich lignin	$C_{15}H_{14}O_4$	
LIG-H	Hydrogen-rich lignin	$C_{22}H_{28}O_9$	
LIG-O	Oxygen-rich lignin	$C_{20}H_{22}O_{10}$	
LIG-CC	Carbon-rich lignin 2	$C_{15}H_{14}O_4$	
LIG-OH	OH-rich lignin	$C_{19}H_{22}O_8$	
G{CO <sub>2</sub> }	Trapped CO <sub>2</sub>	CO <sub>2</sub>	
G{CO}	Trapped CO	CO	
G{COH <sub>2</sub> }	Trapped COH <sub>2</sub>	CH <sub>2</sub> O	
G{H <sub>2</sub> }	Trapped H <sub>2</sub>	H <sub>2</sub>	
Char	Char	C	
<i>Volatiles</i>			
AA/HAA	Acetic acid/hydroxyacetaldehyde	$C_2H_4O_2$	Carbonyls + alcohols
GLYOX	Glyoxal	$C_2H_2O_2$	Carbonyls + alcohols
C <sub>3</sub> H <sub>6</sub> O	Propanal (acetone)	$C_3H_6O$	Carbonyls + alcohols
C <sub>3</sub> H <sub>4</sub> O <sub>2</sub>	Propanedial	$C_3H_4O_2$	Carbonyls + alcohols
HMFU	5-Hydroxymethyl-furfural	$C_6H_6O_3$	Furans
LVG	Levogluconan	$C_6H_{10}O_5$	Sugars
XYL	Xylose monomer	$C_5H_8O_4$	Sugars
pCOUMARYL	Paracoumaryl alcohol	$C_9H_{10}O_2$	Phenolics
PHENOL	Phenol	$C_6H_6O$	Phenolics
FE2MACR	Sinapaldehyde	$C_{11}H_{12}O_4$	Phenolics
H <sub>2</sub>	Hydrogen	H <sub>2</sub>	Permanent gases
CO	Carbon monoxide	CO	Permanent gases
CO <sub>2</sub>	Carbon dioxide	CO <sub>2</sub>	Permanent gases
CH <sub>4</sub>	Methane	CH <sub>4</sub>	Permanent gases
CH <sub>2</sub> O	Formaldehyde	CH <sub>2</sub> O	Carbonyls + alcohols
CH <sub>3</sub> OH	Methanol	CH <sub>4</sub> O	Carbonyls + alcohols
C <sub>2</sub> H <sub>4</sub>	Ethylene	C <sub>2</sub> H <sub>4</sub>	Permanent gases
CH <sub>3</sub> CHO	Acetaldehyde	$C_2H_4O$	Carbonyls + alcohols
ETOH	Ethanol	$C_2H_6O$	Carbonyls + alcohols
H <sub>2</sub> O	Water vapour	H <sub>2</sub> O	Water vapour

Acetic acid is also included in the initial composition of hemicellulose from hardwoods and softwoods and it is released in the first hemicellulose reaction (R5). The main hemicellulose macromolecule of hardwoods is acetylglucuronoxylan [15], usually composed of 10 xylose molecules, 7 acetyl groups and 1 glucuronic acid [16]. The acetyl groups represent in this case around 15% of the mass. In the original scheme hemicellulose is represented by xylan ( $C_5H_8O_4$ ). In the adapted scheme, hardwood hemicellulose is represented by 10 xylan molecules ( $C_5H_8O_4$ ) per 4 acetic acid ( $C_2H_4O_2$ , AA in Table 1 and Fig. 1) ones, so that the acetic acid molecules represent around 15% of the initial mass. The CHO (carbon, hydrogen and oxygen) contents of the new representative hemicellulose molecule (HCEHW) are almost not affected.

The hemicellulose scheme in the original Ranzi scheme is based on xylan, which is actually a better representative for hemicelluloses of hardwoods than softwood. Hemicellulose in softwood is

composed of galactoglucomanan, glucomannan and arabinoglucuronoxylan [16,17]. A reaction scheme based on glucomannan would be more appropriate for softwoods; however, it is not yet available. Hemicelluloses of softwoods are also acetylated, although to a lower extent than for hardwood. Glucomannan is usually composed of 4 hexose sugar monomers and 1 acetyl group [16]. The acetyl groups represent in this case around 4.5% of the mass. In the adapted scheme, softwood hemicellulose (HCESW) is represented by 10 xylan molecules ( $C_5H_8O_4$ ) per 1 acetic acid ( $C_2H_4O_2$ , AA in Table 1 and Fig. 1), so that the acetic acid molecules represent around 4.5% of the initial mass. However, the degree of acetylation varies significantly for softwood [16], which can lead to uncertainties. The influence of employing xylan as a representative for softwoods will be later analysed.

It is proposed by the group of Ranzi to calculate the initial composition of each species based on the CHO contents provided by the elemental analysis [18]. But this approach is very sensitive to small experimental errors, as differences in CHO contents among biomass types are not large [19]. Therefore, another approach is followed here. A representative composition is taken for hardwood and softwood, shown in Table 3. These compositions will be employed for all simulations in this work. The mean value of the range reported in literature for lignin is selected [20]: 22% mass (18–25%) for hardwood and 30% mass (25–35%) for softwood. Cellulose content is set to 44% mass [20] for hardwood and softwood and the hemicellulose content is obtained by difference. The lignin composition (LIG-C, LIG-H and LIG-O) is calculated for the mean values for hardwood and softwood species reported by Faravelli et al. [21]. Softwood lignin is richer in LIG-C due to its higher carbon content.

**Table 3**  
Modeled composition of hardwood and softwood in ash-free % mass.

	Hardwood	Softwood
Cellulose	44.0	44.0
Hemicellulose	34.0	26.0
LIG-C	6.0	17.5
LIG-H	7.0	9.5
LIG-O	9.0	3.0
Total lignin	22.0	30.0
% C	48.6	51.0
% H	6.0	6.0
% O	45.4	43.0

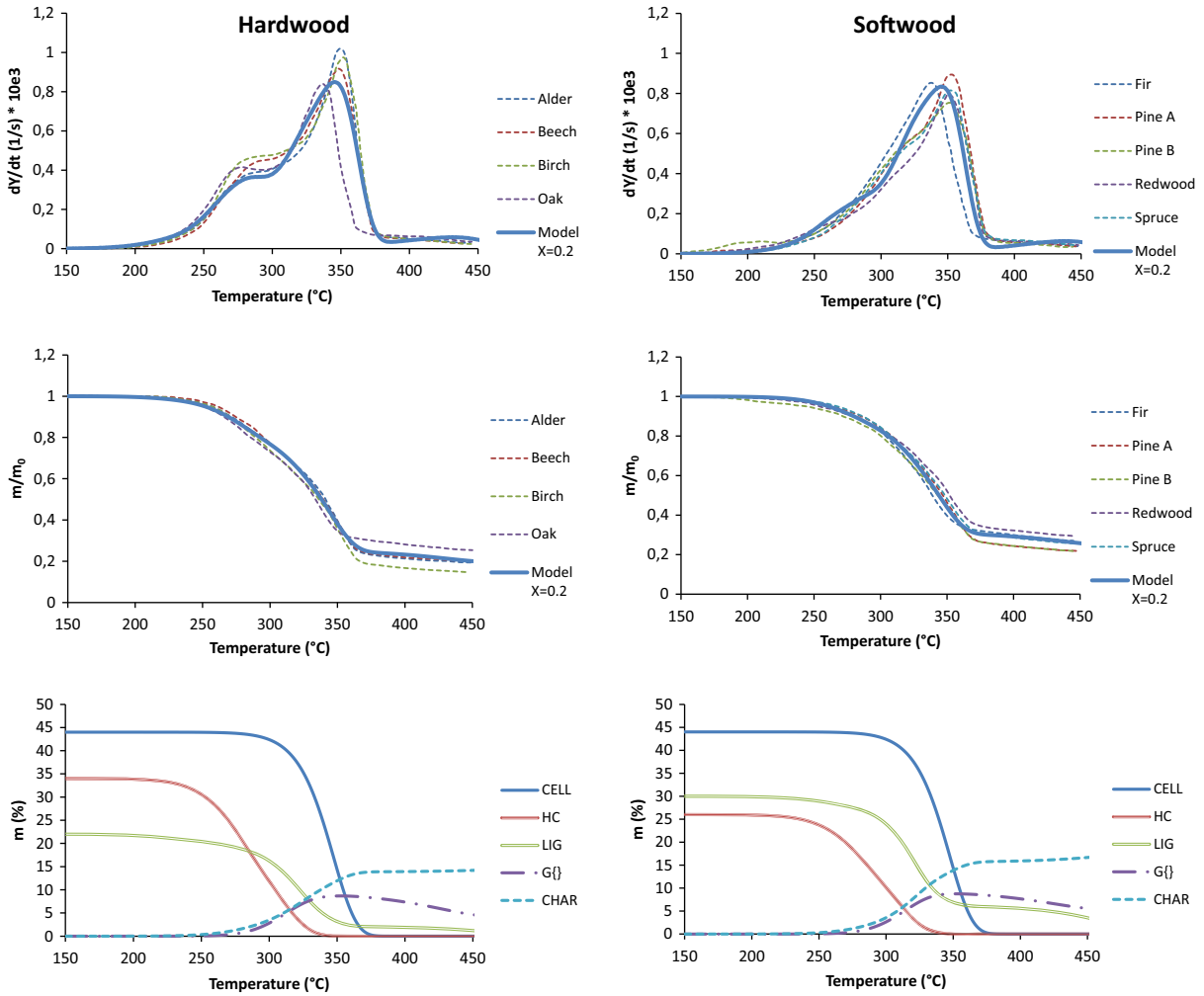


Fig. 2. Experiments [22] and model predictions of reaction rates (top,  $dY/dt$ , being  $Y = m/m_0$ ,  $m$  mass and  $t$  time) and mass loss (middle) over temperature of pyrolysis at 5 K/min with hardwood (left) and softwood (right) species. The evolution of cellulose, hemicellulose, lignin, char and G{ forms predicted by the model is shown at the bottom.

### 3. Mass loss evolution

A general kinetic scheme should predict differences in pyrolysis and torrefaction of diverse biomass types. This work aims to predict the differences in mass loss between hardwood and softwood species. Hardwood and softwood have a different mass loss behaviour during pyrolysis, especially at low temperatures, which is very relevant for torrefaction. Gronli et al. [22] conducted micro thermo-gravimetric experiments at 5 K/min with initial masses of 5 mg of 4 hardwood and 5 softwood species. The adapted scheme is applied with the parameter “ $x$ ”, representing the amount of secondary charring reactions, equal to 0.2 in order to match the final char yield. This parameter is lower than the value employed for pyrolysis of particles in the cm range at similar heating rates in typical fixed bed conditions ( $x = 0.3–0.4$ ). The reason is the lower particle size, i.e., powder, in these micro-TGA experiments, which leads to less secondary charring reactions.

The scheme can correctly predict the mass loss evolution for hardwood and softwood species in these conditions, as seen in Fig. 2. The reaction rate at lower temperatures of softwoods is lower due to the lower hemicellulose content and differences in lignin composition. Softwood contains more LIG-C, which reacts at higher temperatures, and less LIG-H and LIG-O, which react at lower temperatures. The char yield of softwood is higher as lignin, especially LIG-C, produces more char.

As torrefaction is actually a partial pyrolysis process, a pyrolysis kinetic scheme should be also valid for torrefaction. The adapted kinetic is applied in Fig. 3 to predict torrefaction experiments conducted by Prins et al. [3] with willow (hardwood) at different temperatures. Experiments start at 200 °C with a mass sample lower than 10 mg (powder) and the target temperature is achieved at a heating rate of 10 K/min; afterwards the temperature is kept constant. The model is applied with the parameter “ $x$ ” equal to 0.2, as

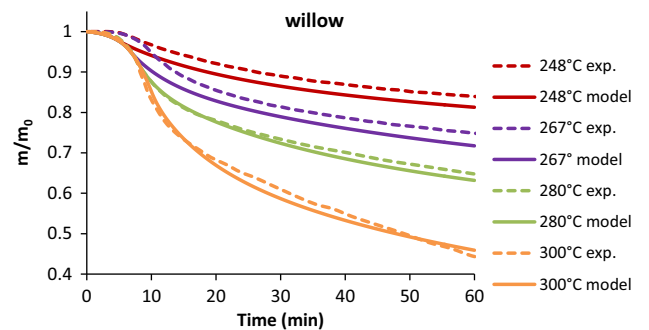


Fig. 3. Experiments [3] and model predictions for torrefaction of willow (hardwood) at different temperatures.

**Table 4**  
Elemental analysis, ash and moisture content of employed fuels.

	Beech chips (hardwood)	Spruce chips (softwood)
C (% mass d.b.)	48.44	50.14
H (% mass d.b.)	6.03	6.16
O (% mass d.b.)	44.46	43.22
N (% mass d.b.)	0.12	0.06
Ash (% mass d.b.)	0.95	0.42
Moisture (% mass w.b.)	6.4	5.2

previously. Good agreement is found between the model and experimental results. The agreement is excellent for the torrefaction experiments at higher temperatures. The experimental mass loss starts slightly later than model predictions for the

low temperature experiments. We can conclude that mass loss of lignocellulosic biomass torrefaction can be also predicted with this detailed kinetic scheme, although certain deviations are present at very low temperatures. Corbetta et al. [14] have already shown that the Ranzi scheme is able to predict mass loss evolution of cellulose, hemicellulose and lignin under torrefaction conditions.

#### 4. Product composition

##### 4.1. Experimental results

The product composition predicted by the scheme is going to be compared to experimental torrefaction results obtained with a batch lab-scale reactor. It consists of a cylindrical retort (0.35 m

**Table 5**  
Experimental (exp.) and model product compositions (original, adapted with  $x=0.3$  and Prins/Bates schemes) in mass percentage of initial wet biomass (w.t.%). LC: light condensable species, HC: heavy condensable species.

	Spruce 250 °C				Beech 250 °C				Beech 285 °C			
	Exp.	Orig.	Adap. $x=0.3$	Prins/bates	Exp.	Orig.	Adap. $x=0.3$	Prins/bates	Exp.	Orig.	Adap. $x=0.3$	Prins/bates
<i>Solid</i>												
Total solid	77.96	82.24	83.29	84.82	71.68	74.07	74.73	77.92	58.01	61.99	63.90	66.15
<i>Permanent gases</i>												
Hydrogen	0.17	0.00	0.06	0.00	0.15	0.00	0.09	0.00	0.12	0.00	0.15	0.00
Carbon monoxide	1.08	0.64	1.23	0.36	1.01	0.79	1.57	0.44	1.65	1.14	2.03	0.63
Carbon dioxide	4.32	1.08	2.08	1.76	4.94	2.10	3.42	2.14	6.46	2.85	4.67	3.07
Methane	0.08	0.53	0.59	0.00	0.13	0.73	0.76	0.00	0.41	1.11	1.07	0.00
Ethylene	0.02	0.48	0.50	0.00	0.01	0.63	0.60	0.00	0.00	0.96	0.84	0.00
Propane	0.00				0.01				0.03			
Propene	0.00				0.29				0.56			
Total permanent gas	5.66	2.72	4.46	2.12	6.54	4.25	6.44	2.57	9.22	6.07	8.75	3.70
<i>Water vapour (LC)</i>												
Total water vapour	9.10	5.88	7.17	9.21	12.46	7.35	9.26	11.64	16.15	8.03	11.46	14.55
<i>Carbonyls + alcohols (mainly LC)</i>												
Formaldehyde	0.67	0.89	0.87		0.28	1.38	1.20		0.32	2.09	1.63	
Acetaldehyde	0.00	0.00	0.06		0.01	0.00	0.13		0.06	0.01	0.40	
Propanal (Acetone)	0.00	0.81	0.89		0.00	0.63	0.79		0.01	0.72	1.24	
Methanol	0.27	0.56	0.58	0.85	0.53	0.91	0.87	2.07	0.86	1.40	1.26	4.38
Ethanol	1.45	0.27	0.28		1.25	0.41	0.39		1.97	0.62	0.52	
Hydroxyacetaldehyde (Acetic acid)	1.56	0.00	1.00	1.54	4.22	0.01	3.93	2.42	6.08	0.05	6.19	4.21
Glyoxal		0.00	0.10			0.00	0.21			0.01	0.66	
Propanedial		0.00	0.00			0.00	0.00			0.00	0.00	
Lactic acid	0.39			0.62	0.27			1.85	0.39			4.14
Formic acid	0.00			0.54	0.00			0.89	0.04			1.60
Hydroxyacetone (HC)				0.21				0.52				1.11
GC detected (HC)	0.58				0.51				0.94			
Total carbonyls + alcohols	4.93	2.52	3.79	3.75	7.09	3.34	7.51	7.76	10.67	4.90	11.89	15.44
<i>(Hetero)cyclics (HC)</i>												
Furfural				0.09				0.11				0.16
5-hydroxymethyl-furfural (HMF)		0.00	0.23			0.01	0.45			0.03	1.43	
GC detected	0.57				0.64				1.29			
Total furans	0.57	0.00	0.23	0.09	0.64	0.01	0.45	0.11	1.29	0.03	1.43	0.16
<i>Sugars (HC)</i>												
Levoglucosan	0.28	1.61	0.00		0.06	3.15	0.00		0.10	9.61	0.00	0.00
Xylose monomer		3.62	0.00			5.60	0.00			5.81	0.00	0.00
Total sugars	0.28	5.23	0.00	0.00	0.06	8.76	0.00	0.00	0.10	15.42	0.00	0.00
<i>Phenolics (HC)</i>												
Paracoumaryl alcohol		0.16	0.16			0.09	0.09			0.14	0.14	
Phenol		0.08	0.08			0.04	0.04			0.07	0.07	
Sinapaldehyde		1.16	0.82			2.10	1.48			3.34	2.35	
GC detected	0.44				0.91				1.80			
Not GC detected	1.06				0.61				2.77			
Total phenolics	1.50	1.40	1.06	0.00	1.53	2.23	1.61	0.00	4.56	3.56	2.57	0.00

height and 0.12 m internal diameter) heated electrically by two separated PID controlled heating circuits. The biomass is put into a cylindrical holder (0.100 m height and 0.095 m i.d.) which is located inside the cylindrical retort. Nitrogen is introduced through a porous plate at the bottom of the fuel bed to keep the system inert and to remove the volatiles. A detailed explanation of the lab-scale reactor was given in a previous publication [23].

Torrefaction of beech chips at 250 and 285 °C and of spruce chips at 250 °C has been investigated. The initial bed weight was 190 g for beech and 75 g for spruce chips and the averaged particle sizes were 12 and 6 mm, respectively. Other properties are stated in Table 4. There is a good agreement between the experimental CHO contents and the ones employed in the model for hardwood and softwood (see Table 3 in comparison to Table 4). Each experiment was conducted two times in order to assure that there is repeatability. The relative deviation in the yields of the main groups that are presented in Table 5 is on average of  $\pm 9\%$ , related to the yield of each group. Temperatures were measured with thermocouples at different heights inside the bed. Since it was impossible to obtain a uniform temperature inside the bed, it has been decided to have the target torrefaction temperature at the middle of the bed. Heating rates in the order of 10 K/min were obtained and the target temperature was kept during approximately 20 min. Mass loss evolution and temperatures in the fuel bed are shown in Fig. 4. The detailed experimental results are available in [24] and results for beech woodchips were previously presented in [13].

Product composition is detailed in Table 5. Volatiles species are classified in permanent gases, light condensable species (LC) and heavy condensable species (HC). The torrgas is extracted from above the fuel bed and the concentrations of permanent gases (including CO, CO<sub>2</sub> and light hydrocarbons) as well as light condensable species were measured by Fourier transform infrared spectroscopy (FT-IR). H<sub>2</sub> was additionally measured by a heat capacity method. Light condensable species are water vapour and several oxygenated species with carbonyl and/or alcohol functional groups. Boiling points of these species range between  $-19$  °C for formaldehyde or 21 °C for acetaldehyde to 118, 122 and 131 °C of acetic acid, lactic acid and hydroxyacetaldehyde, respectively.

In addition, heavy condensable species of the torrgas were measured using a gravimetric method (Tar protocol CEN TC BT/TF 290 143 WICSC 03002.4, 2005) as well as by gas chromatography (GC) coupled to mass spectrometry (MS) to identify the compounds and a flame ionization detector (FID) to quantify them (Agilent 6890 N Network GC System). The tars were sampled in impinger bottles (filled with isopropanol) during the measurements and analysed afterwards in the laboratory. The detected compounds by GC-MS-FID were classified based on their structure in 4 different groups:

- Phenolic compounds: aromatic compounds with a phenyl group, such as guaiacols and syringols.
- (Hetero)cyclic compounds: cyclic compounds, mainly heterocyclics, such as furans (e.g. furfural).
- Carbonyl and/or alcohol compounds: not cyclic compounds with these functional groups, such as hydroxyacetone.
- Sugar compounds: mainly levoglucosan (LGA).

Boiling points of these species are higher than for light condensable species. Values for hydroxyacetone and furfural are 146 °C and 162 °C, respectively. Phenolics, sugars and other (hetero)cyclic compounds have even higher boiling points. The not GC detected fraction of the gravimetric tars is assumed to be pyrolytic lignin [25] to close the balance of gravimetric tars and it is included in the phenolics group. On the contrary to pyrolysis, aromatics without oxygen content (BTX and PAH) are not produced at these low temperatures.

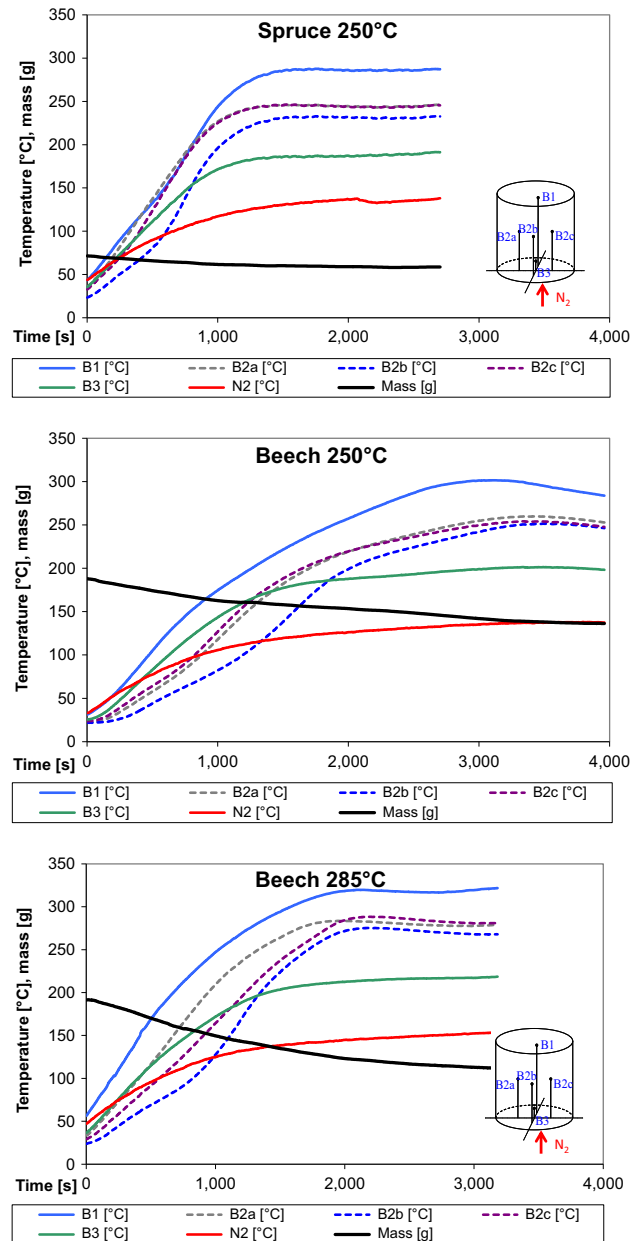


Fig. 4. Mass loss and temperature evolution in the fuel bed during the batch lab-scale torrefaction experiments.

#### 4.2. Model results

The original Ranzi scheme [12], the adapted kinetic scheme presented in Section 2 and the two step kinetic scheme developed by Prins et al. [3] from experiments with willow (hardwood), including the products of each reaction proposed by Bates and Ghoniem [7] (named here Prins/Bates), are applied to describe the experiments. For modelling purposes, the fuel bed is divided into three layers along the height of the bed. The temperature evolutions have been measured for each layer (B1 for the top layer – 90 mm from the bottom; B2a, B2b and B2c for the middle layer – 50 mm from the bottom and 25 mm from the centre for the radial ones – and B3 for the bottom layer – 10 mm from the bottom; see Fig. 4) and the evolutions of the layers are modelled separately by the kinetic model. The entire fuel bed mass loss profile and the final product composition are obtained by a mass weighted average of the results of these three layers, assuming the same ini-

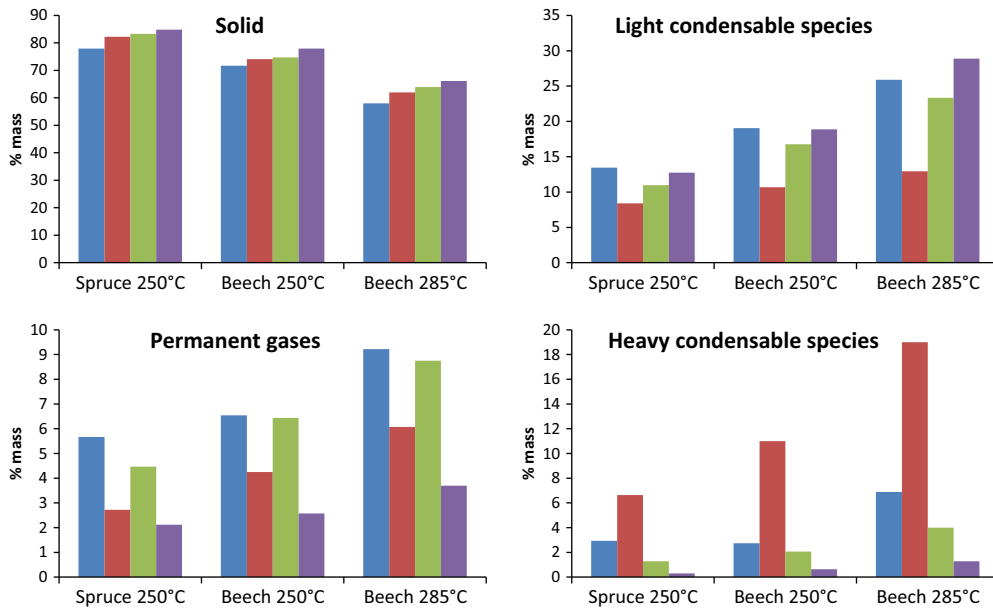


Fig. 5. Product composition of the main groups and species in mass percentage of initial wet biomass.

tial mass for all layers, as explained in Mehrabian et al. [26]. The mass of initial humidity of biomass is included as water vapour in the model predictions, together with the vapour released during torrefaction of the dry biomass. The final product compositions obtained experimentally and by the kinetic schemes are shown in Table 5 and Fig. 5. The adapted scheme is applied with “x” equal to 0.3. The influence of this selection will be later analysed.

The final solid yield is reasonably well predicted by all schemes, considering that a detailed model of heat and mass transfer in the bed is not employed. Slight over-predictions may be caused by higher temperatures achieved near the heated walls than in the position of the thermocouples. Radial temperatures are available for the middle layer, but not for the bottom and top layers. However, significant differences are present in the predictions of the main volatile groups. The original Ranzi scheme predicts very high yields of the sugars levoglucosan and xylose, which leads to a strong over-prediction of the total heavy condensable species. Levoglucosan is found in the experiments, but in minor concentrations. This discrepancy is found because in the original Ranzi scheme the catalytic effect of alkali metals during pyrolysis of cellulose and hemicellulose, dramatically reducing the yields of sugars, is not considered. Moreover, sugars can suffer secondary reactions in contact with char [9]. The experimental yields of sugars were actually lower for beech, with a higher ash content and particle size. On the other hand, the yields of permanent gases, light condensable species (including water vapour and the group of carbonyls and alcohols) as well as (hetero)cyclic compounds are under-predicted by the original scheme. These are main products of fragmentation reactions that are promoted over sugar formation by alkali metals.

The adapted scheme significantly surpasses the other schemes. It has the best predictions of the yields of permanent gases, light and heavy condensable species. Yields of CO, CH<sub>4</sub> and other hydrocarbons are slightly over-predicted while the yield of CO<sub>2</sub> is under-predicted. Regarding light condensable species, the adapted scheme has an accurate prediction of the yield of carbonyls and alcohols due to their formation in fragmentation reactions. Moreover, the yield of acetic acid from beech (hardwood) is correctly predicted due to the inclusion of the production of acetic acid from hemicellulose. The acetic acid yield from spruce (softwood) is however under-predicted. The prediction of the yield of water vapour is

better than for the original scheme, as it is also produced in charring reactions, but remains under-predicted for all cases. Regarding heavy condensable species, it is corroborated by experiments that it is appropriate to eliminate sugar formation in these conditions, as previously discussed. The yield of (hetero)cyclics is well predicted for beech, but under-predicted for spruce; while the yield of phenolics is well predicted for all cases except for the high temperature case for beech.

The main discrepancies between the predictions of the adapted scheme and the experimental results can be explained by the limitations of the adapted scheme. Reactive drying, that takes place at around 200 °C [2] and extractives are not included in the scheme. This may be the reason for the systematic under-prediction of the yields of water vapour, and probably also the one of CO<sub>2</sub>. Hemicellulose is represented in this scheme by xylan, which is appropriate for hardwood. But glucomannan is the main component in hemicellulose from softwood, followed by galactoglucomannan and arabinoglucuronoxylan [27]. Despite the not correct approximation of employing xylan as representative hemicellulose species for softwood, the results for spruce are quite accurate. It was however previously noted that the yields of acetic acid and (hetero)cyclics were under-predicted for this case. Hardwood hemicellulose is strongly acetylated. Softwood hemicellulose is also acetylated, although in a lower proportion [28] and the degree of acetylation varies significantly [16], leading to a higher error. Moreover, a heterocyclic compound (HMFU) is reported to be a main product of softwood hemicellulose but it is not produced from hardwood hemicellulose [29,30]. A more precise description of hemicellulose from softwood would improve the results further. The interactions between biomass components are neither considered in the scheme [31], but this does not seem to hinder significantly its ability to describe torrefaction as the sum of the contributions of cellulose, hemicellulose and lignin. The effects of inorganics are considered to some extent and the presented results are only valid for woody biomass.

The Prins/Bates scheme under-predicts the yields of permanent gases and, especially of heavy condensable species. Heavy condensable species, as phenolics and furans, are produced in significant amounts [32] but are disregarded in many torrefaction studies, as in [8,31]. This scheme predicts correctly the yields of water vapour and carbonyls and alcohols, but under-predicts the

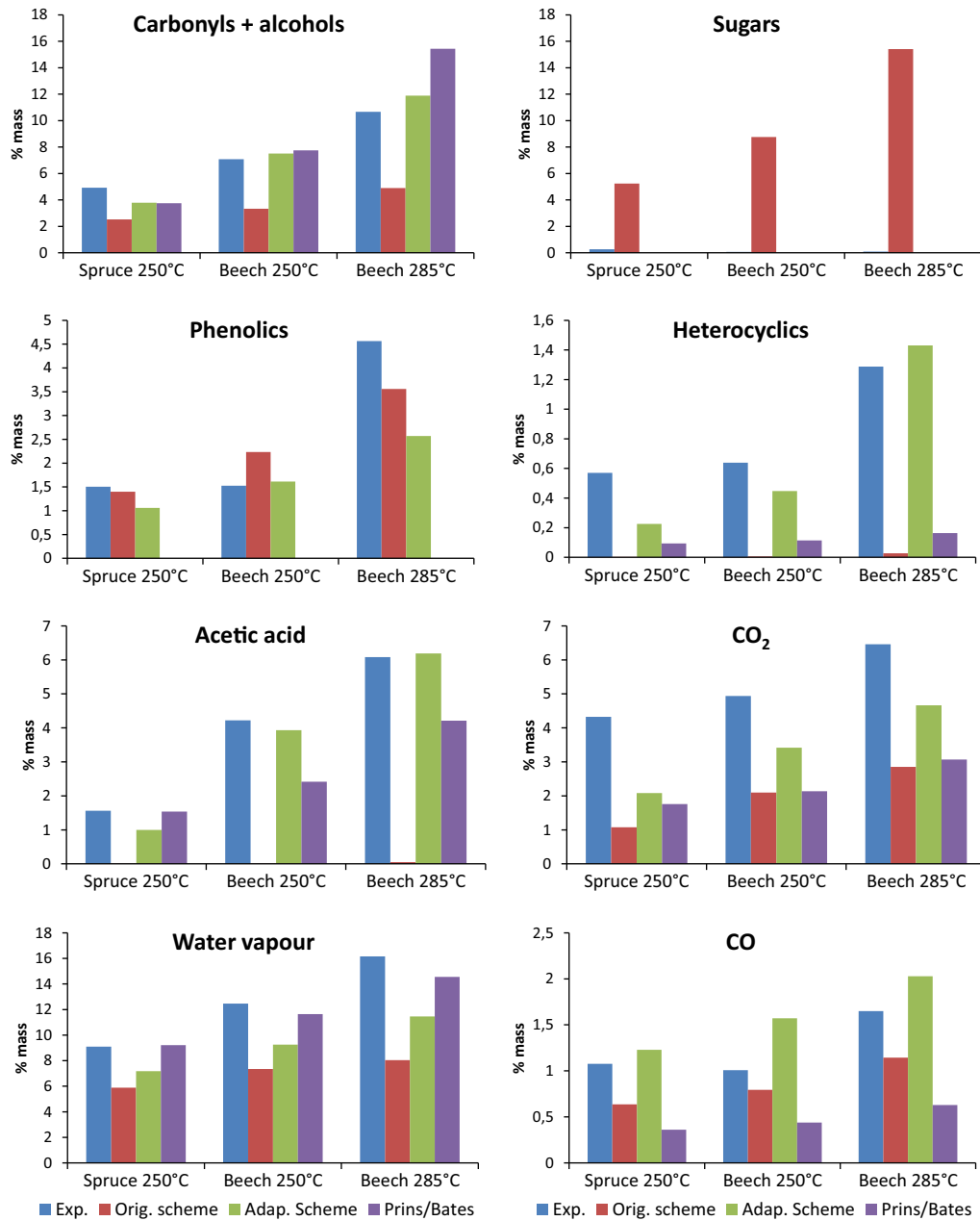


Fig. 5 (continued)

yields of CO and CO<sub>2</sub>. Moreover, it has the limitations previously expounded in Section 1; it cannot be generally applied for lignocellulosic biomass and charring is just a function of the temperature program, not considering other relevant parameters.

Torrefied biomass samples were collected after the experiments from the three layers along the height of the bed and thermogravimetric experiments of the samples were conducted under nitrogen at 20 K/min with an initial mass of 50 mg until a final temperature of 500 °C. The volatile fractions corresponding to cellulose, hemicellulose and lignin have been determined with a fitting routine in the figure plotting the reaction rate ( $dx/dt$ , being  $\alpha$  conversion) over temperature (see Figs. 3 and 4 of Brostrom et al. [33]). Pyrolysis is modelled with a parallel reaction scheme with 3 components representing the devolatilization of cellulose, hemicellulose and lignin. Cellulose and hemicellulose conversion are calculated for each sample, related to the contents of the original biomass, and are plotted in Fig. 6 as a function of the

maximum temperature seen by the sample in the lab-scale reactor. The adapted model can correctly predict the conversion process of hemicellulose at temperatures around 250 °C and the beginning of conversion of cellulose at around 300 °C. There is just an experimental outlier for hemicellulose conversion at the bottom of the bed for the 285 °C experiment with beech, but it is probably caused because higher temperatures are achieved near the heated wall than in the centre of the bed where the thermocouple is placed.

Finally, the influence of variations of the “ $x$ ” parameter on the predictions of the adapted model is checked in Fig. 7 for the experiment with beech at 250 °C. “ $x$ ” is kept constant for all reactions in all cases. When it increases, the yield of total solids and water vapor also increases, as these are the main products of charring reactions. On the other hand, the yields of permanent gases, carbonyls and alcohols, (hetero)cyclics and phenolics decrease, as these are the main reactants of the charring reactions. The minimum averaged error is obtained for “ $x$ ” equal to 0.3 and 0.4 (1.0%

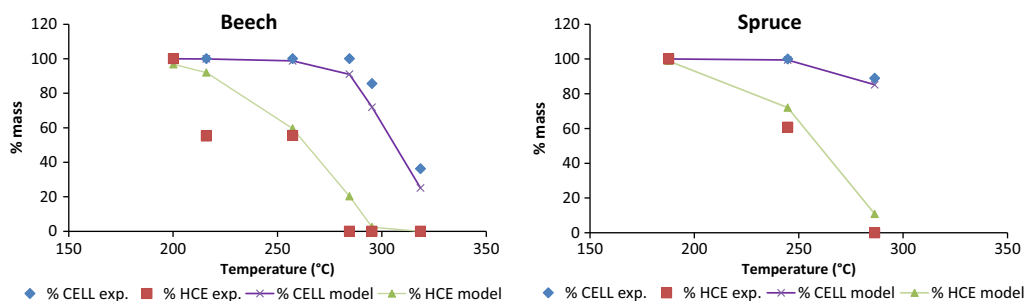


Fig. 6. Cellulose and hemicellulose conversion as a function of the maximum temperature seen by the sample in the lab-scale reactor. Model results obtained with the adapted scheme and “ $x$ ” = 0.3 for all components.

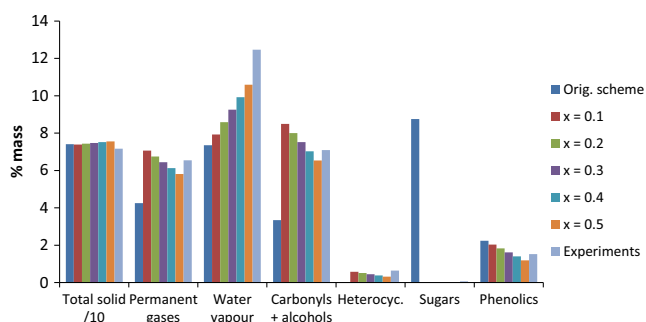


Fig. 7. Comparison of the predictions of the adapted model with different “ $x$ ” values, constant for all reactions in each case, based on the experiments with beech at 250 °C.

error in both cases). Therefore, as for fixed bed pyrolysis, a value in this range is recommended for biomass torrefaction in a fixed bed with particles of around 1 cm and slow heating rates (around 10 K/min). Different values for each component can potentially offer a better description of the process, but there is not enough information available for setting the optimal value for each component currently. The mass loss micro-TGA experiments that have been presented in Section 3 have been modelled with a “ $x$ ” parameter of 0.2. A higher parameter is required to model the lab-reactor experiments due to the higher extent of secondary charring. Moreover, even though slow heating rates have been employed in the lab-scale experiments, intra-particle gradients can be present due to the endothermic drying, heat transfer limitations during the heat-up phase and exothermic reactions afterwards [34]. The “ $x$ ” parameter may to some extent include these phenomena. A more detailed description of the bed of particles would include intra and inter-particle heat and mass transfer phenomena.

## 5. Conclusions and recommendations

A detailed kinetic scheme able to generally predict mass loss evolution and product composition of torrefaction of lignocellulosic biomass is presented in this work. It is a pyrolysis scheme that has been applied in this work to torrefaction, which is actually a partial pyrolysis process. It considers secondary char formation reactions, which are relevant for particles of a certain thickness, and the catalytic effect of alkali metals which avoids sugar formation. Representative initial compositions of hardwood and softwood are proposed and the release of acetic acid from hardwood and softwood hemicellulose is included. The scheme correctly predicts mass loss in micro-TGA pyrolysis and torrefaction experiments and product composition in torrefaction experiments done in a batch lab-scale reactor with beech and spruce. The “ $x$ ” parameter, representing the amount of secondary charring, is set to 0.2

for the micro-TGA experiments. A higher value, in the range from 0.3 to 0.4, is required to describe the fixed bed torrefaction experiments in the lab-scale reactor with particles of woody biomass in the cm range at slow heating rates (around 10 K/min), due to the higher particle size employed in these experiments. Products of torrefaction are classified in permanent gases, light and heavy condensable species. Moreover, the condensable species are classified according to their structure in five groups: carbonyls and alcohols, water vapour, (hetero)cyclics, sugars and phenolics. The scheme predicts with good accuracy the yields of these groups and the main discrepancies can be explained by the limitations of the scheme. Reactive drying at around 200 °C is not included, so the water vapour yield is under-predicted. Moreover, the hemicellulose scheme is based on xylan, which leads to inaccuracies for softwood, such as the under-prediction of the yield of furan compounds. A more precise description of hemicellulose from softwood would include a hemicellulose reaction scheme based on glucomannan and a more precise description of the degree of acetylation. Future work could include the application of the reaction scheme to non woody biomass species and the combination of the detailed reaction scheme with the description of intra and inter-particle heat and mass transfer in a bed of particles.

## References

- [1] van der Stelt MJC, Gerhauser H, Kiel JHA, Ptasiński KJ. *Biomass Bioenergy* 2011;35(9):3748–62.
- [2] Tumuluru JS, Sokhansanj S, Hess JR, Wright CT, Boardman RD. *Ind Biotechnol* 2011;7(5):384–401.
- [3] Prins MJ, Ptasiński KJ, Janssen FJJG. *J Anal Appl Pyrol* 2006;77(1):28–34.
- [4] Repellin V, Govin A, Rolland M, Guyonnet R. *Biomass Bioenergy* 2010;34(5):602–9.
- [5] Ren SJ, Lei HW, Wang L, Bu Q, Chen SL, Wu J. *Biosyst Eng* 2013;116(4):420–6.
- [6] DiBlasi C, Lanzetta M. *J Anal Appl Pyrol* 1997;40:287–303.
- [7] Bates RB, Ghoniem AF. *Bioresour Technol* 2012;124:460–9.
- [8] Prins MJ, Ptasiński KJ, Janssen FJJG. *J Anal Appl Pyrol* 2006;77(1):35–40.
- [9] Anca-Couce A, Mehrabian R, Scharler R, Obernberger I. *Energy Convers Manage* 2014;87:687–96.
- [10] Turner I, Rousset P, Remond R, Perre P. *Int J Heat Mass Transf* 2010;53(4):715–25.
- [11] Tapasvi D, Khalil R, Várhegyi G, Tran KQ, Grønli M, Skreiberg O. *Energy Fuels* 2013;2013(27):6134–45.
- [12] Ranzi E, Cuoci A, Faravelli T, Frassoldati A, Migliavacca G, Pierucci S, et al. *Energy Fuels* 2008;22:4292–300.
- [13] Anca-Couce A, Mehrabian R, Scharler R, Obernberger I. *Chem Eng Trans* 2014;37:43–8.
- [14] Corbetta M, Frassoldati A, Bennadji H, Smith K, Serapiglia MJ, Gauthier G, et al. *Energy Fuels* 2014;28(6):3884–98.
- [15] Moreira LRS, Filho EXF. *Appl Microbiol Biotechnol* 2008;79(2):165–78.
- [16] Patil RA. Cleavage of acetyl groups for acetic acid production in kraft pulp mills. Electronic theses and dissertations, paper 1857, University of Maine; 2012.
- [17] Spiridon I, Popa V. Hemicelluloses: major sources, properties and applications. In: Belgacem MN, Gandini A, editors. *Monomers, Polymers and Composites from Renewable Resources*. Oxford (England): Elsevier; 2008.
- [18] Cuoci A, Faravelli T, Frassoldati A, Granata S, Migliavacca G, Ranzi E, Sommariva S. In: *Proceedings of the 30th combustion meeting of the Italian section of the combustion institute*, vol. VI; 2007. p. 2.1–2.6.
- [19] Vassilev SV, Baxter D, Andersen LK, Vassileva CG. *Fuel* 2010;89(5):913–33.

- [20] Wagenfuhr R, Scheiber C, Holzatlas C, Leipzig Fachbuchverlag; 1974.
- [21] Faravelli T, Frassoldati A, Migliavacca G, Ranzi E. *Biomass Bioenergy* 2010;34:290–301.
- [22] Gronli MG, Varhegyi G, Di Blasi C. *Ind Eng Chem Res* 2002;41:4201–8.
- [23] Brunner T, Biedermann F, Kanzian W, Evic N, Obernberger I. *Energy Fuels* 2013;27(10):5691–8.
- [24] Anca-Couce A, Brunner T, Obernberger I. In: *Proceedings of the 23rd European biomass conference & exhibition*, 1–4 June, Vienna; 2015. p. 1035–41.
- [25] Scholze B, Meier D. *J Anal Appl Pyrol* 2001;60:41–54.
- [26] Mehrabian R, Anca-Couce A, Scharler R, Obernberger I, Janisch W, Trattner K. In: *Proceedings of the 21st European biomass conference & exhibition*, 3–7 June, Copenhagen; 2013. p. 879–86 [ISSN: 2282-5819].
- [27] Branca C, Di Blasi C, Mango C, Hrablay I. *Ind Eng Chem Res* 2013;52(14):5030–9.
- [28] Candelier K, Chaouch M, Dumarcay S, Petrisans A, Petrisans M, Gerardin P. *J Anal Appl Pyrol* 2011;92(2):376–83.
- [29] Di Blasi C, Branca C, Galgano A. *Ind Eng Chem Res* 2010;49(6):2658–71.
- [30] Raisanen U, Pitkanen I, Halttunen H, Hurtt M. *J Therm Anal Calorim* 2003;72(2):481–8.
- [31] Nocquet T, Dupont C, Commandre JM, Grateau M, Thiery S, Salvador S. *Energy* 2014;72:188–94.
- [32] Zheng AQ, Zhao ZL, Chang S, Huang Z, He F, Li HB. *Energy Fuels* 2012;26(5):2968–74.
- [33] Brostrom M, Nordin A, Pommer L, Branca C, Di Blasi C. *J Anal Appl Pyrol* 2012;96:100–9.
- [34] Bates RB, Ghoniem AF. *Fuel* 2014;137:216–29.